



Tau decay into ν_τ and $a_1(1260)$, $b_1(1235)$, and two $K_1(1270)$

L. R. Dai^{1,2,3,a}, L. Roca^{4,b}, E. Oset^{3,c}

¹ School of Science, Huzhou University, Huzhou 313000, Zhejiang, China

² Department of Physics, Liaoning Normal University, Dalian 116029, China

³ Departamento de Física Teórica and IFIC, Centro Mixto Universidad de Valencia-CSIC, Institutos de Investigación de Paterna, Aptdo. 22085, 46071 Valencia, Spain

⁴ Departamento de Física, Universidad de Murcia, 30100 Murcia, Spain

Received: 21 May 2020 / Accepted: 7 July 2020 / Published online: 25 July 2020

© The Author(s) 2020

Abstract We study the $\tau \rightarrow \nu_\tau A$ decay, with A an axial-vector meson. We produce the $a_1(1260)$ and $b_1(1235)$ resonances in the Cabibbo favored mode and two $K_1(1270)$ states in the Cabibbo suppressed mode. We take advantage of previous chiral unitary approach results where these resonances appear dynamically from the vector and pseudoscalar meson interaction in s-wave. Actually two different poles were obtained associated to the $K_1(1270)$ quantum numbers. We find that the unmeasured rates for $b_1(1235)$ production are similar to those of the $a_1(1260)$ and for the two K_1 states we suggest to separate the present information on the $\bar{K}\pi\pi$ invariant masses into $\bar{K}^*\pi$ and ρK modes, the channels to which these two resonances couple most strongly, predicting that these modes peak at different energies and have different widths. These measurements should shed light on the existence of these two K_1 states. In addition, we have gone one step further making a comparison with experimental results of three meson decay channels, letting the vector mesons of our approach decay into pseudoscalars, and we find an overall good agreement with experiment.

1 Introduction

Tau decays, with about 65 % branching fraction into hadronic channels [1], (being the τ the only lepton with enough mass to decay into hadrons), have proved to be a good tool to learn about strong interactions at low energies [2–5]. In particular, some of the decay modes have one resonance in the final state and we are concerned about the production of particular resonances which stand for a molecular interpretation. Concretely, in this work we are concerned about the production

of axial vector resonances, A , this is, $\tau \rightarrow \nu_\tau A$. Given that in the $\tau \rightarrow \nu_\tau q\bar{q}$ at the quark level, the quarks are $d\bar{u}$ for the Cabibbo favored process, this defines the hadronic state with isospin $I = 1$. Hence, we can obtain the $a_1(1260)$ ($1^-(1^{++})$) and the $b_1(1235)$ ($1^+(1^{+-})$). For Cabibbo suppressed processes the initial quark state is $s\bar{u}$ and hence we produce a state with $I = 1/2$ and strangeness. This is the $K_1(1270)$ ($1/2(1/2^+)$). An issue we wish to raise in this work is the fact that the chiral theories for the axial-vector mesons predict two states for $K_1(1270)$ [6, 7] and we evaluate the rates for decay into either state and suggest the way to differentiate the two states in experiment. In chiral unitary theory, the axial vector mesons are generated from the interaction of vector mesons with pseudoscalars [6, 8, 9]. The production of an axial-vector meson in the tau decay proceeds then in the following way: all possible pairs of vector-pseudoscalar are produced and then they are allowed to interact among themselves, and in this process the resonances are generated, decaying later on in vector-pseudoscalar pairs or other channels. From the microscopical point of view this is done from the original $q\bar{q}$ pair creation by means of hadronization, where an extra $\bar{q}q$ pair is created with the quantum numbers of the vacuum. A technical way to implement this step is done in Ref. [10] using the 3P_0 model [11–13] and we shall use some results from this work here.

In the literature there are many works dealing with the production of vector-pseudoscalar in tau decays using different approaches. In Refs. [14, 15] vector meson dominance is used while in Refs. [16–23] the Nambu Jona Lasinio model (NJL) [24] is used. In those works the axial resonances when suited, are introduced explicitly via amplitudes dictated by symmetries [14, 15] or with explicit coupling to quarks in the NJL model. This is different to our approach, since what we do is produce the vector-baryon pairs and then, using chiral dynamics and coupled channels Bethe Salpeter equations the pairs are allowed to interact and the interaction generates the

^a e-mail: dailianrong68@126.com

^b e-mail: luisroca@um.es (corresponding author)

^c e-mail: oset@ific.uv.es

axial-vector resonances, which are implicit in the scattering amplitudes used.

The $\tau \rightarrow \nu_\tau a_1(1260)$ has been studied as part of the $\tau \rightarrow \nu_\tau \pi^+ \pi^- \pi^-$, which has had a wide attention experimentally [25–30]. While the $a_1(1260)$ production provides the main contribution to the process, other mechanisms are at work when one wishes to get a very good agreement with experiment [30–41]. Special emphasis in the role of three body unitarity of the final three pion state is made in a recent paper [42]. The $a_1(1260)$ dominance is seen in the $\pi\rho$ decay channel with the ρ identified from the $\pi\pi$ mass distribution.

Contrary to the $a_1(1260)$ production, which has been widely studied, the $b_1(1235)$ production, to the best of our knowledge has not been discussed, neither experimentally nor theoretically. An interesting aspect of the approach we follow is that, since the vector-pseudoscalar channels produced and their weights are very well defined in the tau decay, we can evaluate the production of the different axial-vector mesons with the same approach. This is our aim here, and we shall relate the production of the $a_1(1260)$, $b_1(1235)$ and the two $K_1(1270)$ states. We shall see that the $b_1(1235)$ production rate is of the same order as the $a_1(1260)$ and the two $K_1(1270)$ states are produced with smaller rates, since they are Cabibbo suppressed by a factor about $\tan^2 \theta_c \simeq 1/20$, but they have very distinct decay modes, which we propose to differentiate. The $K_1(1270)$ production has also been reported in the PDG [1,43], but the $K_1(1270)$ is identified by looking at the $K\pi\pi$ mass distribution, which contains both $K^*\pi$ and ρK . According to [7] the two $K_1(1270)$ resonances couple very differently to these two modes, and we suggest that the two modes are separated to visualize the two resonances peaking at different energies and with different widths. Theoretically, the production of the $K_1(1270)$ has also been addressed in [18,20] from the perspective of the Nambu Jona Lasinio model, but only one K_1 state is considered there.

In the present work we shall use results of Ref. [10] and relate the production rates of the four axial vector resonances. The approach of [10] does not calculate absolute rates but just ratios between different production channels. Here we follow the same strategy and relate all the rates with the production of the $a_1(1260)$ resonance. In addition we calculate partial decay rates into different channels to facilitate the experimental work identifying the production of the $b_1(1235)$ and the two $K_1(1270)$ states.

In addition, we have gone one step further and made a comparison of the results, letting the vector mesons decay into pseudoscalars, with the three meson decay channels observed experimentally, finding an overall good agreement with experiment.

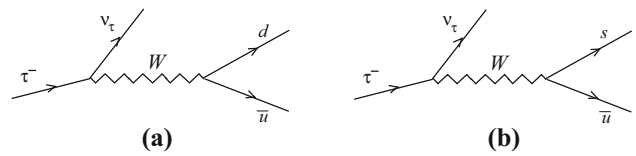


Fig. 1 a Cabibbo favored τ^- decay to quark-antiquark. b Cabibbo suppressed decay

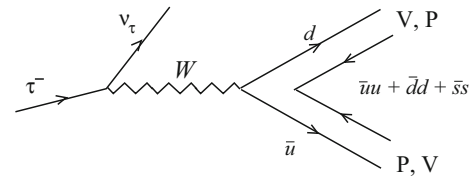


Fig. 2 Hadronization of the primary $q\bar{q}$ pair to produce a vector and pseudoscalar meson

2 Formalism

2.1 Microscopical formalism for meson meson production

Let us begin with the elementary process at the quark level for the τ decay, $\tau \rightarrow \nu_\tau d\bar{u}$ for the Cabibbo favored mode and $\tau \rightarrow \nu_\tau s\bar{u}$ for the Cabibbo suppressed mode. They are depicted in Fig. 1

In order to create a vector and a pseudoscalar meson we introduce a $\bar{q}q$ pair with the quantum numbers of the vacuum. This was done in Ref. [10] using the 3P_0 model. Before one looks into the dynamics of the weak decay, it is easy to see which pairs are created and with which weight. Following Ref. [10] we write the matrix M for $q\bar{q}$,

$$M \equiv \begin{pmatrix} u\bar{u} & u\bar{d} & u\bar{s} \\ d\bar{u} & d\bar{d} & d\bar{s} \\ s\bar{u} & s\bar{d} & s\bar{s} \end{pmatrix}. \tag{1}$$

The hadronization of the $d\bar{u}$ pair is depicted in Fig. 2 and proceeds as

$$d\bar{u} \rightarrow \sum_{i=1}^3 d\bar{q}_i q_i \bar{u} = \sum_{i=1}^3 M_{2i} M_{i1} = (M^2)_{21}. \tag{2}$$

Next we can identify the hadronic states produced with the physical pseudoscalar and vector mesons associating the M matrix to the $SU(3)$ matrices containing the pseudoscalar and vector mesons:

$$M \Rightarrow P \equiv \begin{pmatrix} \frac{\pi^0}{\sqrt{2}} + \frac{\eta}{\sqrt{3}} + \frac{\eta'}{\sqrt{6}} & \pi^+ & K^+ \\ \pi^- & -\frac{1}{\sqrt{2}}\pi^0 + \frac{\eta}{\sqrt{3}} + \frac{\eta'}{\sqrt{6}} & K^0 \\ K^- & \bar{K}^0 & -\frac{\eta}{\sqrt{3}} + \frac{2\eta'}{\sqrt{6}} \end{pmatrix},$$

which makes use of the standard η and η' mixing [44], and

$$M \Rightarrow V \equiv \begin{pmatrix} \frac{1}{\sqrt{2}}\rho^0 + \frac{1}{\sqrt{2}}\omega & \rho^+ & K^{*+} \\ \rho^- & -\frac{1}{\sqrt{2}}\rho^0 + \frac{1}{\sqrt{2}}\omega & K^{*0} \\ K^{*-} & \bar{K}^{*0} & \phi \end{pmatrix}. \quad (3)$$

Then we get the contributions

$$\begin{aligned} (P \cdot V)_{21} &= \pi^- \left(\frac{\rho^0}{\sqrt{2}} + \frac{\omega}{\sqrt{2}} \right) \\ &\quad + \left(-\frac{\pi^0}{\sqrt{2}} + \frac{\eta}{\sqrt{3}} + \frac{\eta'}{\sqrt{6}} \right) \rho^- + K^0 K^{*-}, \\ (V \cdot P)_{21} &= \rho^- \left(\frac{\pi^0}{\sqrt{2}} + \frac{\eta}{\sqrt{3}} + \frac{\eta'}{\sqrt{6}} \right) \\ &\quad + \left(-\frac{\rho^0}{\sqrt{2}} + \frac{\omega}{\sqrt{2}} \right) \pi^- + K^{*0} K^-. \end{aligned} \quad (4)$$

It is important to keep track of the order because the weak transition has two terms and one of them changes sign when changing the order of PV to VP . We shall see that this is directly tied to the G -parity of the states produced. For the Cabibbo suppressed case we proceed analogously but the hadronization of $s\bar{u}$ gives rise to the matrix element $(M^2)_{31}$ with the result

$$\begin{aligned} (P \cdot V)_{31} &= K^- \left(\frac{\rho^0}{\sqrt{2}} + \frac{\omega}{\sqrt{2}} \right) + \bar{K}^0 \rho^- \\ &\quad + \left(-\frac{\eta}{\sqrt{3}} + \frac{2\eta'}{\sqrt{6}} \right) K^{*-}, \\ (V \cdot P)_{31} &= K^{*-} \left(\frac{\pi^0}{\sqrt{2}} + \frac{\eta}{\sqrt{3}} + \frac{\eta'}{\sqrt{6}} \right) + \bar{K}^{*0} \pi^- + \phi K^-. \end{aligned} \quad (5)$$

The next ingredient is the evaluation of the weak interaction operators. The weak interaction is given by the product of the lepton and quark currents

$$H = \mathcal{C} L^\mu Q_\mu, \quad (6)$$

where in \mathcal{C} , which we take constant, we include weak interaction couplings and radial matrix elements of the quark wave functions. These matrix elements are smoothly dependent on the momentum transfer given the small phase space for the reactions, and then, in ratios of rates in which we are interested, the factor \mathcal{C} cancels. (Actually, the difference in the weak coupling between the Cabibbo allowed and suppressed modes will be taken into account later on through the appropriate Cabibbo mixing angle, θ_c). In Eq. (6), $L^\mu Q_\mu$ is the leptonic current

$$L^\mu = \langle \bar{u}_\nu | \gamma^\mu - \gamma^\mu \gamma_5 | u_\tau \rangle, \quad (7)$$

Table 1 Weights h'_i (\bar{h}'_i) of the different $I = 1, G = -1, VP$ components for the M_0 (N_i) amplitudes

	$\rho^0 \pi^-$	$\rho^- \pi^0$	$K^{*0} K^-$	$K^{*-} K^0$
h'_i	0	0	1	1
\bar{h}'_i	$\sqrt{2}$	$-\sqrt{2}$	-1	1

and Q_μ the quark current

$$Q^\mu = \langle \bar{u}_d | \gamma^\mu - \gamma^\mu \gamma_5 | v_{\bar{u}} \rangle. \quad (8)$$

We evaluate the matrix elements in the frame where the resonance is at rest. There $\gamma_5 v = u$ and at these low energies only $\gamma^\mu \rightarrow \gamma^0 \rightarrow 1$ and $\gamma^\mu \gamma_5 \rightarrow \gamma^i \gamma_5 \rightarrow \sigma^i$ survive and we get the components

$$\begin{aligned} Q_0 &= \langle \chi' | 1 | \chi \rangle \equiv M_0, \\ Q_i &= \langle \chi' | \sigma_i | \chi \rangle \equiv N_i, \end{aligned} \quad (9)$$

with $i = 1, 2, 3$, where χ, χ' , are Pauli spinors.

The other point to consider is that, as discussed in [10], the VP mesons are produced in s-wave, unlike PP modes which would be produced in p-wave. This forces the $d\bar{u}$ pair to be produced in $L = 1$ to have positive parity at the end. With the G -parity rule $G = (-1)^{L+S+I}$ ($L = 1, I = 1$, and $S = 0$ for the operator "1" and 1 for the operator σ_i) we see that M_0 carries G -parity positive while N_i carries negative G -parity.

The direct calculation of matrix elements done in [10] using Racah algebra to produce the final meson pair with total angular momentum states $|JM\rangle$ and $|J'M'\rangle$, gives

$$\begin{aligned} M_0(PV) &= M_0(VP) = \frac{1}{\sqrt{6}} \frac{1}{4\pi}, \\ N_\mu(PV) &= -(-1)^{-\mu} \frac{1}{\sqrt{3}} \frac{1}{4\pi} \mathcal{C}(111; M', -\mu, M' - \mu) \delta_{M0}, \\ N_\mu(VP) &= (-1)^{-\mu} \frac{1}{\sqrt{3}} \frac{1}{4\pi} \mathcal{C}(111; M, -\mu, M - \mu) \delta_{M'0}. \end{aligned} \quad (10)$$

It is important to keep in mind that N_i changes sign from the combination PV to VP . This fact is essential to recover the G -parity conservation in the final state interaction, as we shall see. With this rule in mind and Eqs. (4) and (5) one easily finds the weights h'_i, \bar{h}'_i that multiply the M_0 and N_i operators for each of the coupled channels. These factors are shown in Tables 1, 2, 3.

As shown in [10], the differential width for $PV + VP$ production is given by

$$\frac{d\Gamma}{dM_{\text{inv}}(M_1 M_2)} = \frac{2m_\tau 2m_\nu}{(2\pi)^3} \frac{1}{4m_\tau^2} p_\nu \tilde{p}_1 \overline{\sum} \sum |t|^2, \quad (11)$$

Table 2 Same as Table 1 but for $I = 1, G = +1$

	$\omega\pi^-$	$\rho^-\eta$	$K^{*0}K^-$	$K^{*-}K^0$
h'_i	$\sqrt{2}$	$\frac{2}{\sqrt{3}}$	1	1
\tilde{h}'_i	0	0	-1	1

where p_ν is the neutrino momentum in the τ rest frame, and \tilde{p}_1 the momentum of M_1 in the M_1M_2 center of mass frame, and

$$\overline{\sum} \sum |t|^2 = \frac{1}{m_\tau m_\nu} \left(\frac{1}{4\pi}\right)^2 \left[(E_\tau E_\nu + \mathbf{p}^2) \frac{1}{2} |h'_i|^2 + \left(E_\tau E_\nu - \frac{\mathbf{p}^2}{3}\right) |\tilde{h}'_i|^2 \right] \quad (12)$$

where p is the momentum of the neutrino in the rest frame of M_1M_2 and E_τ, E_ν , the energies of the τ and ν_τ for this momentum.

2.2 Final state interaction

As mentioned in the Introduction, the axial-vector resonances are generated in our approach by the interaction of the mesons produced in a first step. Thus we have the mechanism shown in Fig. 3

The dynamics for the WM_1M_2 vertex has been discussed above and the new ingredients are the M_1M_2 loop G function and the couplings of the A_j resonance to the $(M_1M_2)_i$ channels. The information of the G functions is given in [6,7] and the couplings are given in Table VII of [6] for the $a_1(1260)$ and the $b_1(1235)$ resonances, which are obtained from the residues at the pole positions of the VP scattering amplitudes in the proper unphysical Riemann sheets. The couplings for the two K_1 states are given in Table IV in [7]. The position of the poles can be associated with the mass (real part) and width (twice the imaginary part) of the resonances and for the two $K_1(1270)$ states found, that we will call $K_1(A)$ and $K_1(B)$, they are:

$$K_1(A) : M = 1195 \text{ MeV}, \quad \Gamma = 246 \text{ MeV},$$

$$K_1(B) : M = 1284 \text{ MeV}, \quad \Gamma = 146 \text{ MeV}.$$

The first state, $K_1(A)$, couples dominantly to $K^*\pi$ while the second one, $K_1(B)$, couples mostly to ρK . The couplings in

Table 3 Same as Table 1 but for $I = 1/2$. (θ_c is the Cabibbo angle, $\tan \theta_c = 0.2312$)

	$K^{*-}\pi^0$	$\bar{K}^{*0}\pi^-$	ρ^0K^-	$\rho^- \bar{K}^0$	ωK^-	ϕK^-	$K^{*-}\eta$
h'_i	$\frac{1}{\sqrt{2}} \tan \theta_c$	$\frac{1}{\sqrt{2}} \tan \theta_c$	$\frac{1}{\sqrt{2}} \tan \theta_c$	$\tan \theta_c$	$\frac{1}{\sqrt{2}} \tan \theta_c$	$\tan \theta_c$	0
\tilde{h}'_i	$-\frac{1}{\sqrt{2}} \tan \theta_c$	$-\frac{1}{\sqrt{2}} \tan \theta_c$	$\frac{1}{\sqrt{2}} \tan \theta_c$	$\tan \theta_c$	$\frac{1}{\sqrt{2}} \tan \theta_c$	$-\tan \theta_c$	$-\frac{2}{\sqrt{3}} \tan \theta_c$

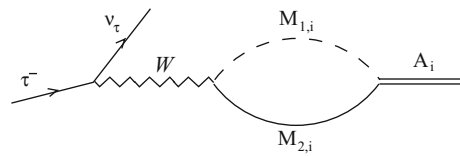


Fig. 3 Mechanism for the production of the dynamically generated axial-vector resonance A_i through the coupled channels $M_{1,i}, M_{2,i}$, of pseudoscalar and vector mesons

Table 4 Couplings of the $I = 1, G = -1$, axial-vector resonance $a_1(1260)$ to the different VP channels

	$\rho^0\pi^-$	$\rho^-\pi^0$	$K^{*0}K^-$	$K^{*-}K^0$
g_i	$\frac{1}{\sqrt{2}} g_{a_1, \rho\pi}$	$-\frac{1}{\sqrt{2}} g_{a_1, \rho\pi}$	$\frac{1}{\sqrt{2}} g_{a_1, K^*\bar{K}}$	$-\frac{1}{\sqrt{2}} g_{a_1, K^*\bar{K}}$

the Tables of Refs. [6,7] are given for the VP isospin states, which are related to the charge states by

$$|\rho\pi; I = 1, I_3 = -1\rangle = \frac{1}{\sqrt{2}} |\rho^0\pi^- \rangle - \frac{1}{\sqrt{2}} |\rho^-\pi^0 \rangle$$

$$|\rho\bar{K}; I = 1/2, I_3 = -1/2\rangle = -\frac{1}{\sqrt{2}} |\rho^0K^- \rangle - \sqrt{\frac{2}{3}} |\rho^-\bar{K}^0 \rangle$$

$$|\bar{K}^*\pi; I = 1/2, I_3 = -1/2\rangle = \frac{1}{\sqrt{3}} |K^{*-}\pi^0 \rangle + \sqrt{\frac{2}{3}} |\bar{K}^{*0}\pi^- \rangle$$

$$|\bar{K}^*K + cc; I = 1, I_3 = -1, G = +1\rangle = -\frac{1}{\sqrt{2}} (|K^{*-}K^0 \rangle + |K^{*0}K^- \rangle)$$

$$|\bar{K}^*K - cc; I = 1, I_3 = -1, G = -1\rangle = -\frac{1}{\sqrt{2}} (|K^{*-}K^0 \rangle - |K^{*0}K^- \rangle) \quad (13)$$

where $\bar{K}^*K \pm cc$ actually stands for the ± 1 G -parity combination $1/\sqrt{2}(K^*\bar{K} \pm \bar{K}^*K)$ [6]. With this information we show in Tables 4, 5, 6 the couplings of a given axial-vector resonance VP channels in terms of the couplings in the isospin basis of Refs. [6,7].

Table 5 Couplings of the $I = 1, G = +1$, axial-vector resonance $b_1(1235)$ to the different VP channels

	$\omega\pi^-$	$\rho^-\eta$	$K^{*0}K^-$	$K^{*-}K^0$
g_i	$g_{b_1,\omega\pi}$	$g_{b_1,\rho\eta}$	$-\frac{1}{\sqrt{2}}g_{b_1,K^*\bar{K}}$	$-\frac{1}{\sqrt{2}}g_{b_1,K^*\bar{K}}$

The amplitude for the mechanism of Fig. 3 is readily obtained simply substituting

$$\begin{aligned}
 h'_j &\rightarrow h''_j = \sum_i h'_i G_i(M_{A_j}) g_{A_j,i} \\
 \bar{h}'_j &\rightarrow \bar{h}''_j = \sum_i \bar{h}'_i G_i(M_{A_j}) g_{A_j,i}
 \end{aligned}
 \tag{14}$$

where i runs over the different coupled channels of each resonance A_j and $g_{A_j,i}$ is the coupling of the A_j resonance to the channel i . The third component of the vectors are easily taken into account. Indeed, the vector propagator keeps the same third component in the WPV vertex and the APV vertex and one must sum over them in the vector propagator. The vertex AVP is of the type $\epsilon_A \cdot \epsilon_V$ [6] and hence one has

$$\sum_{V\text{pol.}} \epsilon_i(V)\epsilon_j(V)\epsilon_j(A) = \delta_{ij}\epsilon_j(A) = \epsilon_i(A) \tag{15}$$

and then the polarization of the axial-vector meson plays the same role as the polarization of the vector meson in the WPV vertex and one evaluates $\overline{\sum} \sum |t|^2$ in the same way as in Eq. (12).

Taking equal masses for the mesons of the same isospin multiplet, the G functions are the same for M_1M_2 independent of the charges and then one can see from Tables 1 and 4 that the M_0 contribution cancels for the a_1 ($G = -$), (h'_i coefficient), but not the N_i contribution, (\bar{h}'_i coefficient), as it should be, since we saw that M_0 has positive G -parity and N_i negative G -parity. Conversely, in the case of the b_1 ($G = +$) it is the N_i part that cancels, (see Tables 2 and 5), as it should be. We see now that the change of sign in N_i implied by Eq. (10) is essential to conserve G -parity in the final state interaction of the mesons. In the case of the $K_1(1270)$ resonances there is no well-defined G -parity but the change of sign implied by Eq. (10) produces particular signs in some channels, which is important for the interference of the different contributions.

Table 6 Couplings of the $I = 1/2$ axial-vector resonances $K_1(A)$ and $K_1(B)$ to the different VP channels. The values of the couplings are different for both poles

	$K^{*-}\pi^0$	$\bar{K}^{*0}\pi^-$	ρ^0K^-	$\rho^- \bar{K}^0$	ωK^-	ϕK^-	$K^{*-}\eta$
g_i	$\frac{1}{\sqrt{3}}g_{K_1,\bar{K}^*\pi}$	$\sqrt{\frac{2}{3}}g_{K_1,\bar{K}^*\pi}$	$-\frac{1}{\sqrt{3}}g_{K_1,\rho\bar{K}}$	$-\sqrt{\frac{2}{3}}g_{K_1,\rho\bar{K}}$	$g_{K_1,\omega\bar{K}}$	$g_{K_1,\phi\bar{K}}$	$g_{K_1,\bar{K}^*\eta}$

To finish the formalism, for the case of the coalescence production that we study, meaning production of the resonance independently of its decay, we have only two particles in the final state and we have the following expression for the width of the $\tau \rightarrow \nu A$ decay:

$$\Gamma(\tau \rightarrow \nu A) = \frac{2m_\tau 2m_\nu}{8\pi} \frac{1}{m_\tau^2} p_\nu \overline{\sum} \sum |t|^2, \tag{16}$$

where we have to use for $\overline{\sum} \sum |t|^2$ the same expression as in Eq. (12) with the substitutions given in Eq. (14) and p_ν the momentum of the neutrino in the tau rest frame and p the momentum of the neutrino in the A rest frame.

3 Partial decay widths

In order to ease comparison with experimental data we will also estimate the branching ratios to final VP states. In order to do that, we can multiply the τ decay width into an axial-vector resonance by its branching ratio into an specific VP channel,

$$\Gamma(\tau \rightarrow \nu_\tau A \rightarrow \nu_\tau VP) = \Gamma(\tau \rightarrow \nu_\tau A) \frac{\Gamma(A \rightarrow VP)}{\Gamma_A}, \tag{17}$$

with

$$\Gamma(A \rightarrow VP) = \frac{|g_{A,VP}|^2}{8\pi M_A^2} q. \tag{18}$$

where $g_{A,VP}$ are the couplings of the axials to the specific final VP channel, (see Tables 4, 5, 6).

In order to take into account the finite width of the axial and the vector mesons, we fold Eq. (17) with their corresponding mass distributions provided by the spectral functions of the axial, $\rho_A(s_A)$, and vector meson $\rho_V(s_V)$,

$$\begin{aligned}
 \Gamma(\tau \rightarrow \nu_\tau A \rightarrow \nu_\tau VP) &= \frac{1}{\mathcal{N}} \int_{(M_A-2\Gamma_A)^2}^{(M_A+2\Gamma_A)^2} ds_A \int_{(M_V-2\Gamma_V)^2}^{(M_V+2\Gamma_V)^2} ds_V \\
 &\cdot \rho_V(s_V)\rho_A(s_A)\Gamma(\tau \rightarrow \nu_\tau A \rightarrow \nu_\tau VP)(\sqrt{s_A}, \sqrt{s_V}) \\
 &\cdot \Theta(\sqrt{s_A} - \sqrt{s_V} - M_P)\Theta(m_\tau - \sqrt{s_A}),
 \end{aligned} \tag{19}$$

where Θ is the step function and Γ_A and Γ_V are the axial and vector mesons total width. In Eq. (19), \mathcal{N} is the normalization of the spectral distribution:

$$\mathcal{N} = \int_{(M_A-2\Gamma_A)^2}^{(M_A+2\Gamma_A)^2} ds_A \int_{(M_V-2\Gamma_V)^2}^{(M_V+2\Gamma_V)^2} ds_V \rho_V(s_V) \rho_A(s_A) \quad (20)$$

We take for the vector spectral function

$$\rho_V(s_V) = -\frac{1}{\pi} \text{Im} \left\{ \frac{1}{s_V - M_V^2 + iM_V\Gamma_V} \right\}, \quad (21)$$

and analogously for the axial-vector one, in spite of the fact that for the axial-vector case the shape is not really a Breit-Wigner, but the approximation is good enough given the uncertainties that we will be obtaining in the results. In Eq. (19) $\Gamma(\tau \rightarrow \nu_\tau A \rightarrow \nu_\tau VP)$ in the integrand is to be understood as the $\Gamma(\tau \rightarrow \nu_\tau A \rightarrow \nu_\tau VP)$ explained before but substituting everywhere $M_A \rightarrow \sqrt{s_A}$ and $M_V \rightarrow \sqrt{s_V}$, (except in the VP loop functions, G , which already had its own consideration of the finite vector meson widths [6,7]). The convolution is specially relevant in the case where there is little phase space for the decay or it is only possible thanks to the finite width of the particles.

4 Results

We can take one of the branching ratios $\tau \rightarrow \nu_\tau A$ to get the global unknown constant in Eq. (6). For this we take the width $\tau \rightarrow \nu_\tau a_1(1260)$ which can be estimated using the following experimental information: Although the $\tau^- \rightarrow \nu_\tau \pi^+ \pi^- \pi^-$ decay is well studied experimentally, the separation of the axial-vector contribution to the rate is not done since there is interference with non resonant terms. However, if we look up in the PDG [1,2] we find the information

$$BR(\tau^- \rightarrow \nu_\tau a_1(1260) \rightarrow \nu_\tau \pi^- \gamma) = (3.8 \pm 1.5) \times 10^{-4} \quad (22)$$

Together with the other information used in [1,2] in this analysis

$$BR(a_1(1260) \rightarrow \gamma \pi^-) = (2.1 \pm 0.8) \times 10^{-3} \quad (23)$$

thus gives

$$BR(\tau^- \rightarrow \nu_\tau a_1(1260)) = (18 \pm 7) \times 10^{-2}, \quad (24)$$

where we keep the same relative error as in Eq. (22), about 40%, which, according to the analysis of [1,2], already accounts for the error in Eq. (23). The result of Eq. (23) is

Table 7 Branching ratios (in %) for creation of the different axial-vector resonances. The $\tau^- \rightarrow \nu_\tau a_1(1260)$ is fixed to the experimental result as reference

Decay channel	BR (%)
$\tau^- \rightarrow \nu_\tau a_1(1260)$	18 ± 7 (exp)
$\tau^- \rightarrow \nu_\tau b_1(1235)$	10 ± 4
$\tau^- \rightarrow \nu_\tau K_1(A)$	0.63 ± 0.25
$\tau^- \rightarrow \nu_\tau K_1(B)$	0.65 ± 0.26

in good agreement with the theoretical evaluation in [20] of 14%. Although this formation is not necessary for the evaluation done here, concerning the nature of the $a_1(1260)$ as a dynamically generated resonance, evaluations of its radiative decay have been done assuming that nature of the $a_1(1260)$, and using the formalism of the local hidden gauge approach, and a qualitative agreement with data is obtained [45,46], which is improved if some extra genuine component for the $a_1(1260)$ is considered, as done in [47]. Uncertainties from this source can be accommodated within the large errors that our results have.

Normalizing our results to the $a_1(1260)$ production width of Eq. (24), Eq. (16) leads to the results shown in Table 7.

In Tables 8 and 9 we show the branching ratios (in %) for each VP state appearing in the coupled channels in the process $\Gamma(\tau \rightarrow \nu_\tau A \rightarrow \nu_\tau VP)$.

The results of Tables 8 and 9 are illustrative, indicating the channels where one expects larger partial decay widths. In this sense, as usual, the $a_1(1260)$ production has to be searched for in the $\rho\pi$ mode, and the $b_1(1235)$ in the $\omega\pi$ mode. We get a branching ratio $\Gamma(\tau^- \rightarrow \nu_\tau b_1^-(1235) \rightarrow \nu_\tau \omega \pi^-) = (2.3 \pm 1.7)\%$. As we mentioned above, there are no data for this decay mode but the PDG reports a branching ratio for $\tau^- \rightarrow \nu_\tau \omega \pi^-$ of $(1.95 \pm 0.06)\%$. Assuming that this decay mode is dominated by the $b_1(1235)$ one finds good agreement within errors of these results. It would be most interesting to see if the $\omega\pi^-$ mass distribution shows indeed the $b_1(1235)$ peak.

As far as the two $K_1(1270)$ states is concerned, as in [7] and other works that studied the separation of these two states using different reactions [48–50], the suggestion is always the same: to measure the $K^*\pi$ decay mode to see the $K_1(A)$ state and ρK to measure the $K_1(B)$ state. So far experiments look at the $\bar{K}\pi\pi$ invariant mass distribution, which contains both $K^*\pi$ and ρK .

4.1 Comparison with experiment

So far we have made predictions for the production of the $a_1(1260)$, $b_1(1235)$ and the two $K_1(1270)$ states, using as input the a_1 production rate. We also evaluated the partial decay rate into different VP channels. In total we present

Table 8 Branching ratios (in %) for the $\Gamma(\tau \rightarrow \nu_\tau A \rightarrow \nu_\tau VP)$ process for the $I = 1$ intermediate axial-vector resonances. The results have an uncertainty of 40%

Decay channel	$\rho^0\pi^-$	$\rho^-\pi^0$	$\omega\pi^-$	$\rho^-\eta$	$K^{*0}K^-$	$K^{*-}K^0$
$\tau^- \rightarrow \nu_\tau a_1(1260) \rightarrow \nu_\tau VP$	2.7	2.7	–	–	0.03	0.03
$\tau^- \rightarrow \nu_\tau b_1(1235) \rightarrow \nu_\tau VP$	–	–	2.3	0.70	0.23	0.23

Table 9 Branching ratios (in %) for the $\Gamma(\tau \rightarrow \nu_\tau A \rightarrow \nu_\tau VP)$ process for the $I = 1/2$ intermediate axial-vector resonances. The results have an uncertainty of 40%

Decay channel	$K^{*-}\pi^0$	$\bar{K}^{*0}\pi^-$	ρ^0K^-	$\rho^-\bar{K}^0$	ωK^-	ϕK^-	$K^{*-}\eta$
$\tau^- \rightarrow \nu_\tau K_1(A) \rightarrow \nu_\tau VP$	0.12	0.23	0.005	0.010	0.007	0	0
$\tau^- \rightarrow \nu_\tau K_1(B) \rightarrow \nu_\tau VP$	0.019	0.037	0.085	0.17	0.012	0	0.007

26 different rates evaluated with just one experimental input. There is hence plenty of material for experimental confirmation in the future. Yet, at present there is also much experimental information on decays to three pseudoscalar mesons. It is a very educating exercise to take our decay channels and allow the vectors to decay into two mesons, and then compare with the experimental rates for the corresponding three meson decay. Let us take one example, $\tau \rightarrow \nu_\tau \pi^- \bar{K}^0 \pi^0$. We can get this decay channel from Table 9 from $K^{*-}\pi^0 \rightarrow \bar{K}^0 \pi^- \pi^0$, $K^{*0}\pi^- \rightarrow \bar{K}^0 \pi^0 \pi^-$ and $\rho^-\bar{K}^0 \rightarrow \pi^- \pi^0 \bar{K}^0$. Taking into account the Clebsch-Gordan coefficients that take part in the K^* decay into the two possible $K\pi$ modes, we obtain a branching ratio to the $\pi^- \bar{K}^0 \pi^0$ channel of 0.36×10^{-2} . Comparison with the experimental $\tau \rightarrow \nu_\tau \pi^- \bar{K}^0 \pi^0$ assumes that, indeed, the decay is mostly governed by the ρ or K^* intermediate resonant states. We shall make this assumption and compare the results with experiment for all the decays channels that we obtain from Tables 8 and 9. When doing this comparison we are also assuming that the VP states are created via an axial vector current. Assuming that VP are created in s-wave, as we did in [10], leads automatically to this conclusion. In [10] a global analysis of the VP decays convinced us that the VP and VV cases of tau decay proceeded via s-wave, unlike the PP decays that proceeded via p-wave and hence a vector current. The overwhelming dominance of the axial vector current in the VP production processes has been also corroborated in explicit calculations using the Nambu-Jona-Lasinio model in [18, 21–23, 54, 55]. One exception was found in [56] in the study of the $\tau^- \rightarrow \nu_\tau K^{*0} K^-$. In this work the vector current was as big as 50% of the axial vector current which was driven explicitly by the a_1 excitation. We shall come back to this point below.

With these observations we show in Table 10 the results that we obtain for the three pseudoscalar decay modes (or pseudoscalar plus ω or ϕ) that result from the channels we have evaluated. The comparison has been done with the rates

Table 10 Comparison with available experimental [57] branching ratios for three pseudoscalar decay modes (or pseudoscalar plus ω or ϕ)

Decay channel	Experimental BR (%)	This work, BR (%)
$K^-\pi^0\pi^0\nu_\tau$	0.0585 ± 0.0027	0.046
$\pi^-\bar{K}^0\pi^0\nu_\tau$	0.3807 ± 0.0124	0.36
$K^-\pi^0K^0\nu_\tau$	0.1494 ± 0.0070	0.17
$\pi^-K^0\bar{K}^0\nu_\tau$	0.1516 ± 0.0247	0.17
$K^-\pi^+\pi^-\nu_\tau$	0.2923 ± 0.0067	0.27
$\pi^-K^-K^+\nu_\tau$	0.1431 ± 0.0027	0.17
$K^-\pi^0\eta\nu_\tau$	0.00483 ± 0.00116	0.0023
$\pi^-\bar{K}^0\eta\nu_\tau$	0.00936 ± 0.00149	0.0047
$K^-\omega\nu_\tau$	0.0410 ± 0.0092	0.019
$K^-\phi\nu_\tau$	0.0044 ± 0.0016	0
$\pi^-\omega\nu_\tau$	1.955 ± 0.063	2.3

$\mathcal{B}_{23}, \mathcal{B}_{40}, \mathcal{B}_{42}, \mathcal{B}_{46}, \mathcal{B}_{93}, \mathcal{B}_{130}, \mathcal{B}_{132}, \mathcal{B}_{151}, \mathcal{B}_{167}, \mathcal{B}_{80}$ and \mathcal{B}_{802} of the HFLAV averages [57]. We have excluded the three pion decay mode, which as we have discussed in the Introduction contains many elements and has been widely discussed in the literature. We find a relatively good agreement in eight of these decay rates, much better than expected in view of the admitted 40% uncertainties in the theory. The agreement is also remarkable given the fact that the results in Table 10 span three orders of magnitude. We get a rate about one half the experimental one for the case of the $K^-\pi^0\eta$ and the related one $\bar{K}^0\pi^-\eta$. Here one can argue that the $\pi\eta$ system will combine to produce the $a_0(980)$ resonance, increasing the rate. Hence, getting a smaller number than experiment is consistent with this observation. Note also that the rate of the second mode is about double than the first one, something also obtained in the theory. The $K^-\phi$ mode is zero in our approach, and experimentally it is extremely small, three orders of magnitude smaller than the similar $\pi^-\omega$ case. The $K^-\omega$ decay mode is then the only remaining case where

we obtain about half the experimental rate, but the deviation is about 40% counting experimental errors, of the order of the theoretical uncertainty, and the number is also about two orders of magnitude smaller than for the related $K^- \omega$ decay. Thus, we can claim an overall good agreement with the experimental branching ratios considering the assumptions we made. At this point we come back to the results of [56], where a large contribution from the vector current was obtained which is not considered in our approach. In spite of that we find a very good agreement of our results with experiment in the rates for $K^0 K^- \pi^0$ and $K^- K^+ \pi^-$ decays, which incidentally have the same strength both in the experiment and the theory. The reason is that in [56] the source of the axial current is explicitly tied to the a_1 excitation, and the b_1 excitation is not explicitly considered. What we see in Table 8 is that this decay is dominated by the b_1 excitation and the a_1 strength accounts for only 13%. Thus, assuming even 50% contribution of the vector current relative to the a_1 contribution, as in [56], only changes in 6% our calculation of these rates, and hence, the good agreement found is not surprising.

5 Conclusions

We have studied the reaction $\tau \rightarrow \nu_\tau A$, with A an axial-vector resonance. We find that for the Cabibbo favored decay mode, only the $a_1(1260)$ and $b_1(1235)$ resonances are produced, but the Cabibbo suppressed mode produces two $K_1(1270)$ resonances which have been predicted before. We use an approach in which the axial-vector resonances are dynamically generated from the interaction of pseudoscalar and vector mesons. For the interaction we use the chiral unitary approach. The unitarization in coupled channels of the interaction of these channels, with the only input of the lowest order VP Lagrangians, produces poles for the resonances from where we extract the residues, and hence the couplings of the resonances to the different channels, which are basic ingredients in the present quantitative calculation. The weak interaction part is handled by a direct evaluation of the weak matrix elements at the quark level and using the 3P_0 model to hadronize the primary $q\bar{q}$ pair formed in the tau decay. We evaluate decay rates relative to one of the decay mode, for which we take experimental data on the $\tau \rightarrow \nu_\tau a_1(1260)$. We obtain rates for the $b_1(1235)$ production which are similar to those of the $a_1(1260)$ production and suggest to see this mode in the $\tau^- \rightarrow \nu_\tau \omega \pi^-$ decay. For the case of the two $K_1(1270)$ states we show that they should be looked upon in different channels, the lower mass state should be seen in the $\bar{K}^* \pi$ mode, while the K_1 state of higher mass should appear in the ρK decay mode. We note that experiments looking for this resonance measure so far the $\bar{K}^* \pi$ invariant mass that contains both the $\bar{K}^* \pi$ and the ρK modes. A separa-

tion of these two channels should show two different peaks with a different width, as predicted by the theory and confirmed with other experiments [7]. Collecting more statistics in present facilities and with the advent of planned ones, the Hefei project in China [51], another one in Novosibirsk [52], and the Belle II update [53], there will be opportunities to have a look at the issues discussed here and learn more about important aspects of Hadron dynamics, in particular the nature of hadronic resonances.

We also evaluated the rates for the decay products into three pseudoscalar mesons and found a very good overall agreement with data. This gives further strength to our predictions and should be an extra stimulus to find the resonant contributions that we have evaluated.

Acknowledgements LRD acknowledges the support from the National Natural Science Foundation of China (Grant Nos. 11975009, 11575076). This work is partly supported by the Spanish Ministerio de Economía y Competitividad and European FEDER funds under Contracts No. FIS2017-84038-C2-1-P B and No. FIS2017-84038-C2-2-P B. This project has received funding from the European Union's Horizon 2020 research and innovation programme under Grant Agreement No. 824093 for the STRONG-2020 project.

Data Availability Statement This manuscript has no associated data or the data will not be deposited. [Authors' comment: All data generated during this study are contained in this published article.]

Open Access This article is licensed under a Creative Commons Attribution 4.0 International License, which permits use, sharing, adaptation, distribution and reproduction in any medium or format, as long as you give appropriate credit to the original author(s) and the source, provide a link to the Creative Commons licence, and indicate if changes were made. The images or other third party material in this article are included in the article's Creative Commons licence, unless indicated otherwise in a credit line to the material. If material is not included in the article's Creative Commons licence and your intended use is not permitted by statutory regulation or exceeds the permitted use, you will need to obtain permission directly from the copyright holder. To view a copy of this licence, visit <http://creativecommons.org/licenses/by/4.0/>. Funded by SCOAP³.

References

1. M. Tanabashi et al., [Particle Data Group]. Phys. Rev. D **98**, 030001 (2018)
2. S. Schael et al., [ALEPH Collaboration]. Phys. Rept. **421**, 191 (2005)
3. M. Davier, A. Hocker, Z. Zhang, Rev. Mod. Phys. **78**, 1043 (2006)
4. E. Braaten, S. Narison, A. Pich, Nucl. Phys. B **373**, 581 (1992)
5. G.D. Lafferty, Nucl. Part. Phys. Proc. **260**, 247 (2015)
6. L. Roca, E. Oset, J. Singh, Phys. Rev. D **72**, 014002 (2005)
7. L.S. Geng, E. Oset, L. Roca, J.A. Oller, Phys. Rev. D **75**, 014017 (2007)
8. M.F.M. Lutz, E.E. Kolomeitsev, Nucl. Phys. A **730**, 392 (2004)
9. Y. Zhou, X. Ren, H. Chen, L. Geng, Phys. Rev. D **90**(1), 014020 (2014)
10. L.R. Dai, R. Pavao, S. Sakai, E. Oset, Eur. Phys. J. A **55**, 20 (2019)
11. L. Micu, Nucl. Phys. B **10**, 521–526 (1969)

12. A. Le Yaouanc, L. Oliver, O. Pene, J.C. Raynal, Phys. Rev. D **8**, 2223 (1973)
13. F. E. Close. in *An Introduction to Quarks and Partons*, (Academic Press, London, 1979), ISBN: 9780121751524
14. B.A. Li, Phys. Rev. D **52**, 5165–5183 (1995)
15. B.A. Li, Phys. Rev. D **52**, 5184–5193 (1995)
16. M. Volkov, A. Arbuzov, D. Kostunin, Phys. Rev. D **86**, 057301 (2012)
17. M. Volkov, A. Arbuzov, Phys. Usp. **60**(7), 643–666 (2017)
18. M. Volkov, A. Pivovarov, JETP Lett. **108**(6), 347–351 (2018)
19. M. Volkov, K. Nurlan, A. Pivovarov, JETP Lett. **106**(12), 771–774 (2017)
20. M. Volkov, K. Nurlan, Phys. Part. Nucl. Lett. **14**(5), 677–680 (2017)
21. M. Volkov, A. Pivovarov, K. Nurlan, Eur. Phys. J. A **55**(9), 165 (2019)
22. M. Volkov, A. Pivovarov, JETP Lett. **110**(4), 237–241 (2019)
23. M. Volkov, A. Pivovarov, K. Nurlan, Nucl. Phys. A **1000**, 121810 (2020)
24. Y. Nambu, G. Jona-Lasinio, Phys. Rev. **122**, 345–358 (1961)
25. R. Barate et al., [ALEPH.] Eur. Phys. J. C **4**, 409–431 (1998)
26. I. M. Nugent, SLAC-R-936, Doctorate Thesis, SLAC Stanford National Laboratory
27. R.A. Briere et al., [CLEO]. Phys. Rev. Lett. **90**, 181802 (2003)
28. B. Aubert et al., [BaBar]. Phys. Rev. Lett. **100**, 011801 (2008)
29. M. Lee et al., [Belle]. Phys. Rev. D **81**, 113007 (2010)
30. I. Nugent, T. Przedzinski, P. Roig, O. Shekhovtsova, Z. Was, Phys. Rev. D **88**, 093012 (2013)
31. Y. Ivanov, A. Osipov, M. Volkov, Z. Phys. C **49**, 563–568 (1991)
32. M. Bowler, Phys. Lett. B **182**, 400–404 (1986)
33. N. Isgur, C. Morningstar, C. Reader, Phys. Rev. D **39**, 1357 (1989)
34. G. Colangelo, M. Finkemeier, R. Urech, Phys. Rev. D **54**, 4403–4418 (1996)
35. D. Dumm, P. Roig, A. Pich, J. Portoles, Phys. Lett. B **685**, 158–164 (2010)
36. Z. Was, J. Zaremba, Eur. Phys. J. C **75**(11), 566 (2015)
37. J.J. Sanz-Cillero, O. Shekhovtsova, JHEP **12**, 080 (2017)
38. Z. Guo, Phys. Rev. D **78**, 033004 (2008)
39. M. Wagner, S. Leupold, Phys. Rev. D **78**, 053001 (2008)
40. M. Wagner, S. Leupold, Phys. Lett. B **670**, 22–26 (2008)
41. A. Osipov, Phys. Rev. D **99**(3), 034023 (2019)
42. M. Mikhasenko et al. [JPAC], Phys. Rev. D **98**(9), 096021 (2018)
43. R. Barate et al., [ALEPH]. Eur. Phys. J. C **11**, 599–618 (1999)
44. A. Bramon, A. Grau, G. Pancheri, Phys. Lett. B **283**, 416–420 (1992)
45. L. Roca, A. Hosaka, E. Oset, Phys. Lett. B **658**, 17–26 (2007)
46. H. Nagahiro, L. Roca, A. Hosaka, E. Oset, Phys. Rev. D **79**, 014015 (2009)
47. H. Nagahiro, K. Nawa, S. Ozaki, D. Jido, A. Hosaka, Phys. Rev. D **83**, 111504 (2011)
48. L.R. Dai, L. Roca, E. Oset, Phys. Rev. D **99**, 096003 (2019)
49. G. Wang, L. Roca, E. Oset, Phys. Rev. D **100**(7), 074018 (2019)
50. G. Wang, L. Roca, E. Wang, W. Liang, E. Oset, Eur. Phys. J. C **80**, 388 (2020)
51. Q. Luo and D. R. Xu, in *Proceedings of the 9th International Particle Accelerator Conference*. <https://doi.org/10.18429/JACoW-IPAC2018-MOPML013>
52. S. Eidelman, Nucl. Part. Phys. Proc. **260**, 238–241 (2015)
53. E. Kou et al. [Belle-II], PTEP **2019**(12), 123C01 (2019)
54. M.K. Volkov, A.A. Pivovarov, K. Nurlan, [arXiv:1903.00698](https://arxiv.org/abs/1903.00698) [hep-ph]
55. M. K. Volkov and A. A. Pivovarov, Pisma Zh. Eksp. Teor. Fiz. **109**, 219 (2019) [JETP Lett. **109**, no. 4, 222 (2019)] Erratum: [JETP Lett. **109**, no. 12, 821 (2019)]
56. M.K. Volkov, A.A. Pivovarov, K. Nurlan, Inter. J. Mod. Phys. A **35**, 2050035 (2020)
57. Y. S. Amhis et al. [HFLAV], [arXiv:1909.12524](https://arxiv.org/abs/1909.12524) [hep-ex]